Fault detection in dynamic processes using a simplified monitoring-specific CVA state space modelling approach

Shallon Stubbs, Jie Zhang, Julian Morris
Centre for Process Analytics and Control Technology
School of Chemical Engineering and Advanced Materials, Newcastle University,
Newcastle upon Tyne NE1 7RU, UK
E-mail: shallon.stubbs@ncl.ac.uk; jie.zhang@ncl.ac.uk; julian.morris@ncl.ac.uk

Abstract

State space models have been successfully used for the modelling, control and monitoring of dynamic processes with several different approaches employed to derive the state variables of the model. Typically, state-space canonical variate analysis (CVA) modelling requires the estimation of five matrices to fully parameterize the model. This paper proposes a simpler CVA state space model defined by three matrices for the specific purpose of process monitoring. A modified definition of the past vector of inputs and output is proposed in order to facilitate efficient estimation of a reduced set of state space matrices. A sequential procedure for accurate selection of the model state vector dimension is also proposed. The proposed method is applied to the benchmark Tennessee Eastman process and the results show that the proposed method gives comparable and in some cases even better performance than the established CVA state space monitoring methods.

Keywords: state space modelling, CVA, dynamic models, fault detection, process monitoring.

1. Introduction

State space models have been reported to be superior to other multivariate statistical methods for the modelling, control and monitoring of dynamic processes. In the area of system identification and predictive modelling, Juricek et al. (2005) demonstrated that subspace models based on canonical variate analysis (CVA) and numerical algorithm for subspace identification (N4SID) outperformed regression models based on partial least squares (PLS) and constraint categorical regression (CCR). They also demonstrated that, of the two subspace modelling methods, the CVA model was more accurate than its N4SID counterpart. Other comparative analysis works carried out by Simoglou et al. (1999a) and Negiz and Cinar (1997b)

have also provided support for the superior performance of CVA based state space models.

A few variants of the state space model representations have also been explored and presented in the literature. Typically, the form of CVA based state-space representation is one that can be used in applications ranging from process modelling, control and monitoring. Such a model generally requires the estimation of five matrices to fully parameterize the model. In control system applications this representation is necessary as control of the plant is achieved via methods involving the application of calculated input signal(s) based upon the past output measurements. Thus far very little emphasis has been placed on selecting a state-space model based upon its intended application and most if not all recent papers employing state space models for process monitoring applications have resorted to this full model representation (Lee et al., 2006; Yao and Gao, 2008; Odiowei and Cao, 2010).

This paper proposes an adaptation of the state space model representation and CVA based derivation for the specific purpose of process monitoring. The proposed state space model employs a significantly reduced number of parameters. The reduced dimensionality of the model, in conjunction with a slightly amended method of constructing the past vector, makes the model parameter estimation much simpler and more efficient.

The proposed model is used for process monitoring and applied to the benchmark Tennessee Eastman (TE) process under close-loop control. Process monitoring is carried out using the Hotelling's T^2 statistics and squared prediction error (SPE, also known as Q) statistics of the state and output residuals. The results are compared with the reported fault detection performance from previous publications (Russell et al., 2000; 2007), where the same set of 21 faults are used. Russell et al. (2000) evaluated three different fault detection models: the traditional CVA state space modelling technique, standard and dynamic principal component analysis (PCA and DPCA), whereas Detroja et al. (2007) evaluated the detection performance of the Hotelling's T^2 statistics and Q statistics based upon a statistical method called correspondence analysis (CA). Results from these previous publications show that the traditional CVA state space model gives overall the best performance. The results of this paper

demonstrates that the proposed CVA state space model can offer at least the same and in some cases better fault detection performance in terms of fault detection delay time compared to the traditional CVA state space model.

The paper is organised as follows: Section 2 presents the modified CVA based state space model and highlights its differences from those pioneered by Akaike (1975) and Larimore (1990). Section 3 delves into the application of several model selection criterions and how they were employed for the selection of the appropriate state vector dimension used to construct the state space model. Section 4 introduces the fault monitoring statistics employed and Section 5 provides a comparative analysis and summary of the results obtained alongside that of previous publications. Some conclusions are drawn in Section 6.

2. State space modelling and canonical variate analysis

2.1 Conventional and the proposed CVA based state space models

The well known state space model representation is given in Eq. (1). It is premised on the stochastic process exhibiting Markov properties (Akaike, 1975). In the strict sense definition of a Markov process, the future state of the process, that is, the conditional probability of future transitions should only be dependent upon the current state of the process. Hence the proposed representation given by Eq. (2) is not in contradiction to a Markovian representation and quite accurately aligns with the definition.

$$\mathbf{x}_{t+1} = \mathbf{A}\mathbf{x}_t + \mathbf{B}\mathbf{u}_t + \mathbf{e}_x;\ \mathbf{y}_t = \mathbf{C}\mathbf{x}_t + \mathbf{D}\mathbf{u}_t + \mathbf{G}\mathbf{e}_x + \mathbf{e}_y \tag{1}$$

$$\mathbf{x}_{t+1} = \mathbf{A}\mathbf{x}_t + \mathbf{G}\mathbf{e}_y + \mathbf{e}_x\ ;\ \mathbf{y}_t = \mathbf{C}\mathbf{x}_t + \mathbf{e}_y \tag{2}$$

For both state space representation $\mathbf{e}_x$ is the state residuals and $\mathbf{e}_y$ is the uncorrelated output residuals. The respective residuals are of the same vector dimension as the state $\mathbf{x}_t \in \mathbb{R}^k$ and output $\mathbf{y}_t \in \mathbb{R}^{n_y}$ vectors. The proposed state space representation retains the **G** matrix but it is now incorporated in the state transition equation as opposed to the output equation. The **G** matrix is somewhat

similar to the innovation term employed in Kalman filter designs (Brown and Hwang, 1992) where state estimation is iteratively improved by using the innovations or residuals of the output equation. The proposed state space representation, therefore, more closely aligns its representation with that of the Kalman filter design but makes the assumption that the covariance of the measurement data is constant.

According to Larimore (1990), accounting for the correlation between the state and output residual ensures a minimum order hidden Markov state space representation. The proposed state space representation similarly guarantees a minimum order hidden Markov model. However, the size of the state vector is determined via a cross-validation procedure using the state transition equation as opposed to the output equation as is the case for Larimore's model given in Eq. (1).

From a control system point of view the essential difference between the two representations is that the five matrix representation, Eq. (1), explicitly accounts for the input vector $\mathbf{u}_t$ and therefore finds its use in control systems applications. For the purpose of fault and disturbance detection, the proposed model, Eq. (2), would then suffice adequately and even be more desirable, given its advantages in terms of simplification of representation and stochastic estimation equations.

The state space representation Eq. (2) is more concise than Eq. (1) with the removal of the current input vector $\mathbf{u}_t$. In order to retain the information component provided by the input vector $\mathbf{u}_t$, it is proposed here to redefine Larimore's past vector representation and this will be elaborated on in the next subsection.

2.2 Canonical variate analysis and state variable extraction

The main idea behind canonical correlation analysis is to extract the relationship between two sets of variables **X** and **Y** by finding corresponding sets of linear combinations of the original variables (the canonical variates **U** and **V**):

$$\mathbf{U} = \mathbf{XJ} \tag{3}$$

$$\mathbf{V} = \mathbf{YL} \tag{4}$$

The choice of transformation matrices **J** and **L** is towards maximising the correlation between the canonical variates:

$$\max_{\mathrm{J,L}} \frac{\mathbf{J}^{\mathrm{T}}\mathbf{R}_{xy}\,\mathbf{L}}{\sqrt{\mathbf{J}^{\mathrm{T}}\mathbf{R}_{xx}\,\mathbf{J}}\sqrt{\mathbf{L}^{\mathrm{T}}\mathbf{R}_{yy}\,\mathbf{L}}} \tag{5}$$

where $\mathbf{R}_{xx} = E(\mathbf{X}^{\mathrm{T}}\mathbf{X})$, $\mathbf{R}_{yy} = E(\mathbf{Y}^{\mathrm{T}}\mathbf{Y})$, and $\mathbf{R}_{xy} = E(\mathbf{X}^{\mathrm{T}}\mathbf{Y})$.

This is equivalent to solving the following optimization problem:

$$\max_{\mathbf{J,L}} \emptyset = \mathbf{J}^{\mathrm{T}}\mathbf{R}_{xy}\mathbf{L} + \lambda_x(\mathbf{I}_x - \mathbf{J}^{\mathrm{T}}\mathbf{R}_{xx}\mathbf{J}) + \lambda_y\left(\mathbf{I}_y - \mathbf{L}^{\mathrm{T}}\mathbf{R}_{yy}\mathbf{L}\right) \tag{6}$$

where $\mathbf{I}_x$ and $\mathbf{I}_y$ are identity matrices of appropriate dimensions.

The solution is given by:

$$SVD\left(\mathbf{R}_{xx}^{-1/2}\mathbf{R}_{xy}\mathbf{R}_{yy}^{-1/2}\right) = \hat{\mathbf{J}}\mathbf{S}\hat{\mathbf{L}}^{\mathrm{T}} \tag{7}$$

$$\mathbf{J} = \mathbf{R}_{xx}^{-1/2}\hat{\mathbf{J}};\ \ \mathbf{L} = \mathbf{R}_{yy}^{-1/2}\hat{\mathbf{L}} \tag{8}$$

The main diagonal of the **S** matrix contains the correlation coefficients. The combined operation of Eq. (7) and Eq. (8) is referred to as the generalized singular value decomposition (GSVD) of $\mathbf{R}_{xy}$.

For our application, the states are derived as the canonical variates between two sets of variables, one set being the past vector **P** and the other being the future vector **F**, which are traditionally defined as follows:

$$\mathbf{P}_t^T = \left[\mathbf{y}_{t-1}^T;\mathbf{y}_{t-2}^T,\ldots.\mathbf{y}_{t-l_y}^T,\mathbf{u}_{t-1}^T,\mathbf{u}_{t-2}^T,\ldots.\mathbf{u}_{t-l_u}^T\right]^T \tag{9}$$

$$\mathbf{F}_t^T = \left[\mathbf{y}_t^T;\mathbf{y}_{t+1}^T,\ldots.\mathbf{y}_{t+f}^T\right]^T \tag{10}$$

where l_y, l_u, f are, respectively, the numbers of lags in the output, input, and the number of lead elements of the output samples in the future vector.

The state vector $\mathbf{x}_t$ is computed from the canonical variate transform **J** of the past vector:

$$\mathbf{x}_t = \mathbf{J}\mathbf{P}_t^T \; ; \; \text{GSVD}\left(\mathbf{R}_{pf}\right) = \mathbf{J}\mathbf{S}\mathbf{L}^{\text{T}} \tag{11}$$

subject to $\mathbf{J}^{\text{T}}\mathbf{R}_{pp}\mathbf{J} = \mathbf{I}_m$ and $\mathbf{L}^{\text{T}}\mathbf{R}_{ff}\mathbf{L} = \mathbf{I}_q$, where $\mathbf{R}_{pp} = \mathbf{P}^{\text{T}}\mathbf{P}$, $\mathbf{R}_{pf} = \mathbf{P}^{\text{T}}\mathbf{F}$, and $\mathbf{R}_{ff} = \mathbf{F}^{\text{T}}\mathbf{F}$.

To account for the removal of the $\mathbf{u}_t$ input in the proposed state space representation, the following definition of the past vector **P** is proposed in this paper:

$$\mathbf{P}_t^T = \left[\mathbf{y}_{t-1}^T; \mathbf{y}_{t-2}^T, \ldots . \mathbf{y}_{t-l_y}^T, \mathbf{u}_t^T, \mathbf{u}_{t-1}^T, \ldots . \mathbf{u}_{t-l_u}^T\right]^T \tag{12}$$

The subtle amendment is the inclusion of the $\mathbf{u}_t$ vector in the past matrix definition such that the process of deriving the states would retain what information that is contained by the input vector at the current time $\mathbf{u}_t$.

2.3 Estimating parameters in the state space model

Larimore's stochastic estimation procedure is summarised by Eq. (13) to Eq. (16). The stochastic algorithms first derives estimates for the matrices **A**, **B**, **C**, and **D** and then proceeds to simultaneously derive the covariance matrices of the state and output residuals ($\mathbf{\Phi}_x$, $\mathbf{\Phi}_y$) along with the parameters of the **G** matrix:

$$\begin{bmatrix} \widehat{\mathbf{A}} & \widehat{\mathbf{B}} \\ \widehat{\mathbf{C}} & \widehat{\mathbf{D}} \end{bmatrix} = \begin{bmatrix} \mathbf{x}_{t+1}^T\mathbf{x}_t & \mathbf{x}_{t+1}^T\mathbf{u}_t \\ \mathbf{y}_t^T\mathbf{x}_t & \mathbf{y}_t^T\mathbf{u}_t \end{bmatrix} \begin{bmatrix} \mathbf{x}_t^T\mathbf{x}_t & \mathbf{x}_t^T\mathbf{u}_t \\ \mathbf{u}_t^T\mathbf{x}_t & \mathbf{u}_t^T\mathbf{u}_t \end{bmatrix}^{-1} \tag{13}$$

$$\mathbf{e}_x = \mathbf{x}_{t+1} - (\widehat{\mathbf{A}}\mathbf{x}_t + \widehat{\mathbf{B}}\mathbf{u}_t) \tag{14}$$

$$\tilde{\mathbf{y}}_t = \mathbf{y}_t - (\widehat{\mathbf{C}}\mathbf{x}_t + \widehat{\mathbf{D}}\mathbf{u}_t) \tag{15}$$

$$\begin{bmatrix} \mathbf{\Phi}_x & \mathbf{\Phi}_x\mathbf{G} \\ \mathbf{G}^T\mathbf{\Phi}_x & \mathbf{G}^T\mathbf{\Phi}_x\mathbf{G} + \mathbf{\Phi}_y \end{bmatrix} = \begin{bmatrix} \tilde{\mathbf{x}}_{t+1} \\ \tilde{\mathbf{y}}_t \end{bmatrix} [\tilde{\mathbf{x}}_{t+1} \quad \tilde{\mathbf{y}}_t]^T \tag{16}$$

where $\mathbf{\Phi}_x = \mathbf{e}_x^{\text{T}}\mathbf{e}_x$, $\mathbf{\Phi}_y = \mathbf{e}_y^{\text{T}}\mathbf{e}_y$ and the total output equation residuals $\tilde{\mathbf{y}}_t = \mathbf{G}\mathbf{e}_x + \mathbf{e}_y$.

The stochastic estimation algorithm developed for the alternative three matrix representation presented in this paper produces a much simpler set of equations based upon minimizing the squared residuals of the state and output equations.

We shall now expand Eq. (13) to illuminate the hidden computation complexity of Larimore's stochastic algorithm when applied to the CVA modelling approach using a five matrices state space model representation. We begin by first deriving the inverse matrix term appearing in Eq. (13):

$$\begin{bmatrix} \mathbf{x}_t^T\mathbf{x}_t & \mathbf{x}_t^T\mathbf{u}_t \\ \mathbf{u}_t^T\mathbf{x}_t & \mathbf{u}_t^T\mathbf{u}_t \end{bmatrix} \begin{bmatrix} \mathbf{S}_{11} & \mathbf{S}_{12} \\ \mathbf{S}_{21} & \mathbf{S}_{22} \end{bmatrix} = \begin{bmatrix} \mathbf{I} & 0 \\ 0 & \mathbf{I} \end{bmatrix} \tag{17}$$

From manipulation of Eq. (17) the following results can be derived:

$$\mathbf{S}_{21} = -[\mathbf{u}_t^T\mathbf{u}_t]^{-1}\mathbf{u}_t^T\mathbf{x}_t\mathbf{S}_{11} \tag{18}$$

$$\mathbf{S}_{12} = -[\mathbf{x}_t^T\mathbf{x}_t]^{-1}\mathbf{x}_t^T\mathbf{u}_t\mathbf{S}_{22} \tag{19}$$

$$\mathbf{S}_{11} = [\mathbf{x}_t^T\mathbf{x}_t - \mathbf{x}_t^T\mathbf{u}_t[\mathbf{u}_t^T\mathbf{u}_t]^{-1}\mathbf{u}_t^T\mathbf{x}_t]^{-1} \tag{20}$$

$$\mathbf{S}_{22} = [\mathbf{u}_t^T\mathbf{u}_t - \mathbf{u}_t^T\mathbf{x}_t[\mathbf{x}_t^T\mathbf{x}_t]^{-1}\mathbf{x}_t^T\mathbf{u}_t]^{-1} \tag{21}$$

Finally, returning to Eq. (13) the estimates of the state matrices can now be obtained:

$$\begin{bmatrix} \widehat{\mathbf{A}} & \widehat{\mathbf{B}} \\ \widehat{\mathbf{C}} & \widehat{\mathbf{D}} \end{bmatrix} = \begin{bmatrix} \mathbf{x}_{t+1}^T\mathbf{x}_t & \mathbf{x}_{t+1}^T\mathbf{u}_t \\ \mathbf{y}_t^T\mathbf{x}_t & \mathbf{y}_t^T\mathbf{u}_t \end{bmatrix} \begin{bmatrix} \mathbf{S}_{11} & \mathbf{S}_{12} \\ \mathbf{S}_{21} & \mathbf{S}_{22} \end{bmatrix} \tag{22}$$

$$\widehat{\mathbf{A}} = [\mathbf{x}_{t+1}^T\mathbf{x}_t - \mathbf{x}_{t+1}^T\mathbf{u}_t[\mathbf{u}_t^T\mathbf{u}_t]^{-1}\mathbf{u}_t^T\mathbf{x}_t]\mathbf{S}_{11} \tag{23}$$

$$\widehat{\mathbf{B}} = [\mathbf{x}_{t+1}^T\mathbf{u}_t - \mathbf{x}_{t+1}^T\mathbf{x}_t[\mathbf{x}_t^T\mathbf{x}_t]^{-1}\mathbf{x}_t^T\mathbf{u}_t]\mathbf{S}_{22} \tag{24}$$

$$\widehat{\mathbf{C}} = [\mathbf{y}_t^T\mathbf{x}_t - \mathbf{y}_t^T\mathbf{u}_t[\mathbf{u}_t^T\mathbf{u}_t]^{-1}\mathbf{u}_t^T\mathbf{x}_t]\mathbf{S}_{11} \tag{25}$$

$$\widehat{\mathbf{D}} = [\mathbf{y}_t^T\mathbf{u}_t - \mathbf{y}_t^T\mathbf{x}_t[\mathbf{x}_t^T\mathbf{x}_t]^{-1}\mathbf{x}_t^T\mathbf{u}_t]\mathbf{S}_{22} \tag{26}$$

The computation load in terms of the number of floating point operations required to derive the **A**, **B**, **C**, and **D** matrices based upon Eq. (23) to Eq. (26) is actually less than that required to extract the matrices based upon Eq. (13) because it is computationally cheaper to find the inverse of a $n_u \times n_u$ and a $k \times k$ dimensional matrix separately than to find the inverse of $(n_u + k) \times (n_u + k)$ dimensional matrix. Also, one could employ computation and storage of reusable sub-blocks common to the different equations in the set spanning Eq. (18) to Eq. (26) to further reduce the computation requirements. Nevertheless, either approach would prove computationally more intensive than the reduced set of equations to be derived for the

modified state space modelling approach. The derivation is outlined by Eq. (27) to Eq. (35) and shows how redefining of the past vector **P** and the change in the model representation can lead to a significantly reduced and simplified set of equations.

With reference to Eq. (1), the **B** matrix is derived so as to minimize the squared output residuals:

$$\mathbf{e}_y\mathbf{e}_y^T = \mathbf{y}_t\mathbf{y}_t^T - 2\mathbf{y}_t\mathbf{x}_t^T\mathbf{C}^T + \mathbf{C}\mathbf{x}_t\mathbf{x}_t^T\mathbf{C}^T \tag{27}$$

Note that the state variables of Eq. (1) and Eq. (2) share common properties, in particularly, the covariance of the state vector is still given by an identity matrix as a result of the common CVA procedure employed in extracting the state variables. Applying this special condition to Eq. (27) and setting the derivative function to zero, yields the following results:

$$\frac{d(\mathbf{e}_y\mathbf{e}_y^T)}{d\mathbf{C}} = -2\mathbf{y}_t\mathbf{x}_t^T + 2\mathbf{C} \tag{28}$$

$$\mathbf{C} = \mathbf{y}_t\mathbf{x}_t^T \tag{29}$$

Likewise, the parameters of the **A** and **G** matrices are found from minimizing the squared residuals of the next state equation with respect to **A** and **G**:

$$\mathbf{e}_x\mathbf{e}_x^T = \mathbf{x}_{t+1}\mathbf{x}_{t+1}^T - 2\mathbf{x}_{t+1}\mathbf{x}_t^T\mathbf{A}^\mathbf{T} - 2\mathbf{x}_{t+1}\mathbf{e}_y^T\mathbf{G}^\mathbf{T} + \mathbf{A}\mathbf{x}_t\mathbf{x}_t^T\mathbf{A}^\mathbf{T} + \mathbf{G}\mathbf{e}_y\mathbf{e}_y^T\mathbf{G}^\mathbf{T} + 2\mathbf{A}\mathbf{x}_t\mathbf{e}_y^T\mathbf{G}^\mathbf{T} \tag{30}$$

Eq. (30) can be simplified by setting $\mathbf{x}_t\mathbf{x}_t^T = \mathbf{I}_k$, $\mathbf{x}_{t+1}\mathbf{x}_{t+1}^T = \mathbf{I}_k$ and noting that $\mathbf{x}_t\mathbf{e}_y^T = 0$, these assumptions result in:

$$\boldsymbol{e}_x\boldsymbol{e}_x^T = \mathbf{I}_\mathrm{k} - 2\mathbf{x}_{t+1}\mathbf{x}_t^T\mathbf{A}^T - 2\mathbf{x}_{t+1}\mathbf{e}_y^T\mathbf{G}^T + \mathbf{A}\mathbf{A}^T + \mathbf{G}\mathbf{e}_y\mathbf{e}_y^T\mathbf{G}^T \tag{31}$$

The solutions are obtained by setting the partial derivatives with respect to **A** and **G** to zero:

$$\frac{\partial(\mathbf{e}_x\mathbf{e}_x^T)}{\partial\mathbf{A}} = -2\mathbf{x}_{t+1}\mathbf{x}_t^T + 2\mathbf{A} = 0 \tag{32}$$

$$\frac{\partial(\mathbf{e}_x\mathbf{e}_x^T)}{\partial\mathbf{G}} = -2\mathbf{x}_{t+1}\mathbf{e}_y^T + 2\mathbf{e}_y\mathbf{e}_y^T\mathbf{G} = 0 \tag{33}$$

$$\mathbf{A} = \mathbf{x}_{t+1}\mathbf{x}_t^T \tag{34}$$

$$\mathbf{G} = \mathbf{x}_{t+1}\mathbf{e}_y^T\left[\mathbf{e}_y^T\mathbf{e}_y\right]^{-1} \tag{35}$$

Derivation of the state matrices of the proposed simpler model shows that no matrix inversion operation is required to generate the solution for the **A** and **C** matrices of the model.

Table 1 compares the proposed and traditional stochastic estimation algorithms in terms of the numbers of floating point operations (FLOPs) needed to compute the two models. The matrix inversion operation involved in the computation of the A-B and A-B-C-D matrices of the state space models is separately shown so as to highlight its computational load. Online available educational material on matrix inverse computation provided by researchers from the University of South Florida (http://numericalmethods.eng.usf.edu/simulations) demonstrates that matrix inversion operation using LU Decomposition method requires significantly less number of FLOPs over a Gaussian Elimination based technique. The matrix inversion FLOPS given in Table 1 is based on LU decomposition. Note that this serves as a reference for comparison and does not necessarily represent the most efficient inversion considering that the LU decomposition could be substituted for by the Cholesky decomposition. The Cholesky decomposition is a special case of the general LU decomposition that is numerically more stable and efficient than LU decomposition but is applicable only to positive definite symmetric matrices.

Table 1. Computational complexity (FLOPs) of proposed and traditional CVA methods

Computer Operations	Model Type	
	ABG	ABCDG
A to D Matrix: Multiplications and Additions	$2n(n_u n_y + k^2)$	$2n\left[\left(2k + 3n_u + n_y\right)k + \left(n_y + n_u\right)n_u\right] + 2(k + n_u)^3$
A to D Matrix: Matrix Inversion Operation	0	$\frac{4(k+n_u)^3}{3} + \frac{3(k+n_u)^2}{2} - \frac{5(k+n_u)}{6}$
G-Matrix: Computation	$2nn_u\left(k + n_y\right) + \frac{4n_y^3}{3} + \frac{3n_y^2}{2} - \frac{5n_y}{6}$	

n_u – number of inputs; n_y – number of outputs; n – length of training data; k – number of state vectors

3. State matrix sizing and other model considerations

Development of a CVA state space model requires the selection of several sizing parameters: the window lengths of the past and future vectors and the number of state vectors comprising the state matrix. Additionally, consideration must also be given as to whether to apply separate lag/lead order per process variable when constructing the past or future vector.

Simoglou et al. (1999a) presented an overview of several criteria that have been reported in the literature for state vector dimension selection, namely Akaike information criterion (AIC), cross-validation procedures, and selection based on the eigenvalues of the Hankel matrix. In addition to these, there exist several other model order selection criteria such as Final Prediction Error (FPE), Bayesian Information Criterion (BIC), and Law of Iterated Logarithm Criterion (LILC).

AIC is the first of these and the most extensively used in such endeavours. Larimore (1983) proposed using AIC for determination of the lag-order and several other researchers have done likewise (Simoglou et al., 1999a; Juricek et al., 1999). Simoglou et al. (2002) speculated that the use of this common lag order for all the inputs and outputs in the past vector construction may impose some limitations with the use of the method as different variables may exhibit different dynamics and should therefore be included with different numbers of lagged values in the past vector. Negiz and Cinar (1997b) proposed using the autocorrelation trend of the process variables to select the past window lag on a per-variable basis.

The model development carried out in this paper employed a common lag-window size for the past and future vectors. The choice was driven by the need to simplify the model development procedure. To the authors' best knowledge, in the majority of the publications the window lengths for all the process variables were set to the same number of time lags (e.g. Simoglou et al., 1999b; Simoglou et al., 2002; Negiz and Cinar, 1997a). Also, simulation results shown in Fig. 1 indicate that the choice of lag-window size is not very critical to the accuracy of the developed model and that the state vector size selection is a more influential factor. This result was based upon simulation data using a multi-input multi-output (MIMO) autoregressive

model with exogenous input (ARX), defined by Eq. (36) to Eq. (38). The ARX time series model employed for the simulation is an expanded and more involved version of the single-input two-output ARMAX time series model used by Negiz and Cinar (1997a). Additive measurement noise with a signal to noise ratio of 10% is added to input and output measurements. The model simulates three output signals from three independent inputs:

$$y_1(t) = 0.95y_1(t-1) - 0.35y_1(t-2) + 0.8u_1(t) \tag{36}$$

$$y_2(t) = 0.35y_2(t-1) + u_1(t) + 0.4u_2(t) \tag{37}$$

$$y_3(t) = 0.6y_1(t-1) - 0.3y_2(t-1) + 0.88u_3(t) \tag{38}$$

Both the 3-D contour plot shown in Fig. 1(a) and the family of mean squared error (MSE) plots in Fig. 1(b) demonstrate that the choice of lag window size is of less impact on the performance of the model. Fig. 1(b) also shows that the cross validation MSE plateaus beyond the use of more than three/four states which is consistent with the fact that there are three independent variables in the data set along with one time delayed output term included in the second order time series equation defining output y_1. The MSE plots will later be shown to characterize the shape of the model fitness (maximum likelihood) terms employed by a number of model order selection criteria.

Simoglou et al. (1999b) investigated the noise-sensitivity of several model order selection criteria by observing the impact of measurement noise in the data on the selected model order. They concluded that the most suitable model order was dependent upon the purpose of the model, whether it was employed for prediction or monitoring, and was also dependent upon other specifics about the particular data based model. A list of the criteria investigated in this paper for finding the minimum state vector size is given in Table 2. The list shows that AIC, BIC, and LILC all use the maximum likelihood term to estimate the model fitness and only differ in the term used to quantify model complexity. The maximum likelihood term is itself a function of the covariance of the model residual:

$$\ln p(\mathbf{Y}, \mathbf{U}, \boldsymbol{\Theta}) = Nn_y(\ln 2\pi + \ln\|\mathbf{E}\|) \tag{39}$$

where N is the number of observations, n_y is the number of output variables and $\mathbf{E}$ is the vector of model residuals for the regression model $\mathbf{Y} = \mathbf{U\Theta} + \mathbf{E}$.

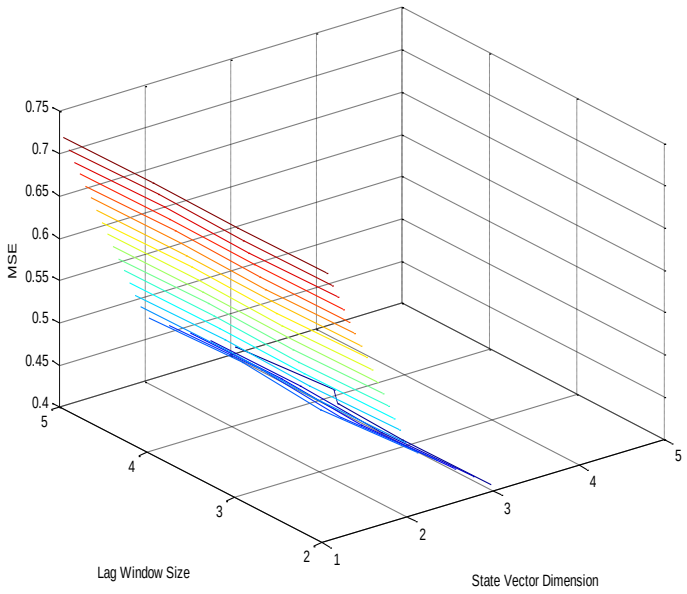

(a)

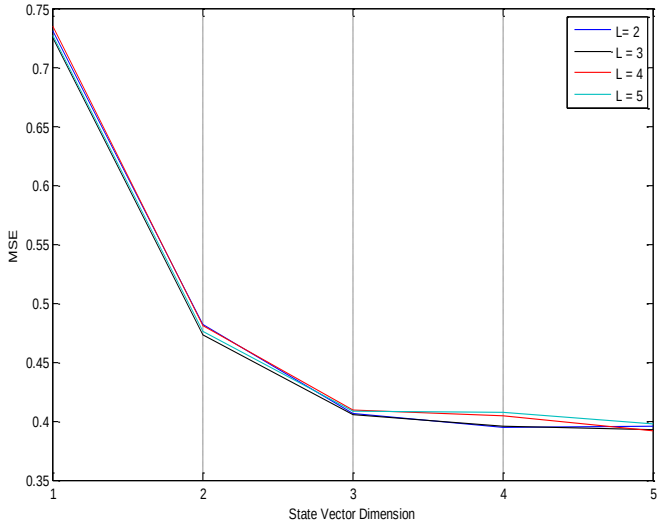

(b)

Fig. 1. a) 3-D plot of model error vs. state vector and lag window sizes; b) Equivalent 2-D family of plots for different lag size L - MSE versus state vector dimension.

Therefore, for a given training data set, the maximum likelihood function is only a logarithmic function of the error covariance of the form:

$$\ln p(\mathbf{Y}, \mathbf{U}, \boldsymbol{\Theta}) = a + b \ln ||\mathbf{E}|| \quad (40)$$

where a and b are constants related to the model training data dimension.

Table 2. A list of model size selection criteria

Criterion	Equation
Akaike Information Criterion - AIC, (Akaike, 1973)	$\mathrm{AIC} = -2 \ln p(\mathbf{Y}, \mathbf{U}, \boldsymbol{\Theta}) + 2m_k$ where m_k is the number of model parameters
Bayesian Information Criterion - BIC, (Hannan and Quinn, 1979)	$\mathrm{BIC} = -2 \ln p(\mathbf{Y}, \mathbf{U}, \boldsymbol{\Theta}) + 2m_k \ln(N)$ where N is the number of observations in the training data set
Law of Iterated Logarithm Criterion - LILC, (Hannan and Quinn, 1979)	$\mathrm{LILC} = -2 \ln p(\mathbf{Y}, \mathbf{U}, \boldsymbol{\Theta}) + 2m_k \ln(\ln N)$
Final Prediction Error - FPE, (Akaike, 1970). The criterion converges towards the AIC for large values of N.	$FPE = N \left[\ln ||E|| + \ln \left(\frac{N + m_k}{N - m_k} \right) \right]$

The desirable parabolic shape obtained when these criteria are employed is therefore a function of the rate or magnitude of decline of the likelihood function curve as the model residual diminishes versus the rate or magnitude of growth of the model complexity term employed as is illustrated in Fig. 2. As such, the point at which the particular criterion employed achieves a minimum (if one is achieved) is subject to the trend of the model residual decline with increasing model parameters and the complexity term employed.

In the case of the proposed CVA state space model, the commonly used equation for computing the number of free parameters, as applied in several papers (Simoglou et al., 1999a; Schaper et al., 1994), is given by:

$$m_k = k(2n_y + n_u) + n_y n_u + n_y(n_y + 1)/2 \quad (41)$$

where k is the number of states, n_u is the number of inputs, and n_y is the number of outputs.

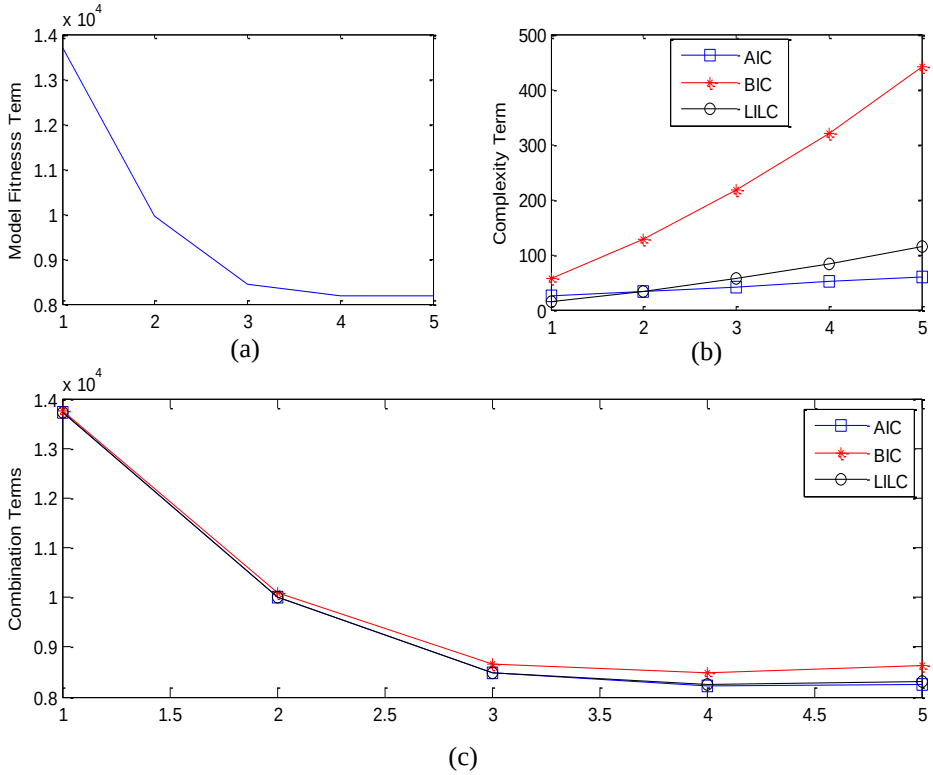

Fig. 2. Plots of the AIC, BIC, LILC criteria dissected in terms of model complexity term and model fitness term

The origin of Eq. (41) is tied to the number of parameters required to parameterize the general state space canonical form which is far less than the number of elements in the various state space matrices (Candy, 1979). However, the numbers of parameters making up the matrices of the proposed state space model versus Larimore's model are given by Eq. (42) and Eq. (43) respectively:

$$m_k = 2kn_y + k^2 \tag{42}$$

$$m_k = k(2n_y + n_u) + n_y n_u + k^2 \tag{43}$$

Due to the large values returned by the likelihood function computation as shown in Fig. 2(a), it is desirable to chose a model complexity term Eq. (41) to Eq. (43) that yields the largest m_k value and the choice as demonstrated previously is therefore

driven by the state space model being employed. The subjective nature of the process therefore requires that the model complexity term be specific to the model so as to guarantee arriving at the true model order. In Fig. 2 the BIC best approximates a parabolic shape with its minimum located at the state order consistent with the observation from the MSE plots in Fig. 1.

An alternative method for identifying the state order of the model is to rely on the MSE cross-validation plots. The stopping criterion employed is based upon a minimum gradient specification:

$$\Delta(k) = \frac{mse(k) - mse(k-1)}{mse(k) - mse(k_{int})} \tag{44}$$

where k is the current state vector size and k_{int} is the initial chosen dimension. The initial state order dimension is typically chosen to be $\min\{n_u, n_y\}$ for the model under evaluation. The final state vector size is then selected when $\Delta(k)$ falls below a pre-determined value, which is typically a small positive value for example 0.01.

The simplification of the state space model parameterization equations facilitates a sequential procedure such that for each past vector window size selected, the state vector size is increased by one in each step until a plateau (minimum gradient change) or minimum point of the MSE plot is detected. The state output error can be updated sequentially for each additional state vector employed by expanding the **C** matrix by a single row when a new state vector is included in the model and then updating the residual vector computation:

i) Compute the kth row-vector of the **C** matrix:
$\mathbf{c}_k^T = \mathbf{Y}_{tr}^T \mathbf{x}_{tr}^k$ where $\mathbf{Y}_{tr}^T$ is an $N \times m$ matrix of training output measurements and $\mathbf{x}_{tr}^k$ is the kth state vector derived as the canonical variate using the training data.
ii) Update the output prediction: $\widehat{\mathbf{Y}}_k = \widehat{\mathbf{Y}}_{k-1} + \mathbf{b}_k \mathbf{x}_v^k$
iii) Update residual matrix: $\mathbf{E}_k = \mathbf{Y}_v - \widehat{\mathbf{Y}}_k$.

Steps (i) to (iii) are repeated until the MSE converges to a minimum value. The state vector dimension and lag-order is then selected based upon the convergence value obtained over the range of past vector window sizes employed.

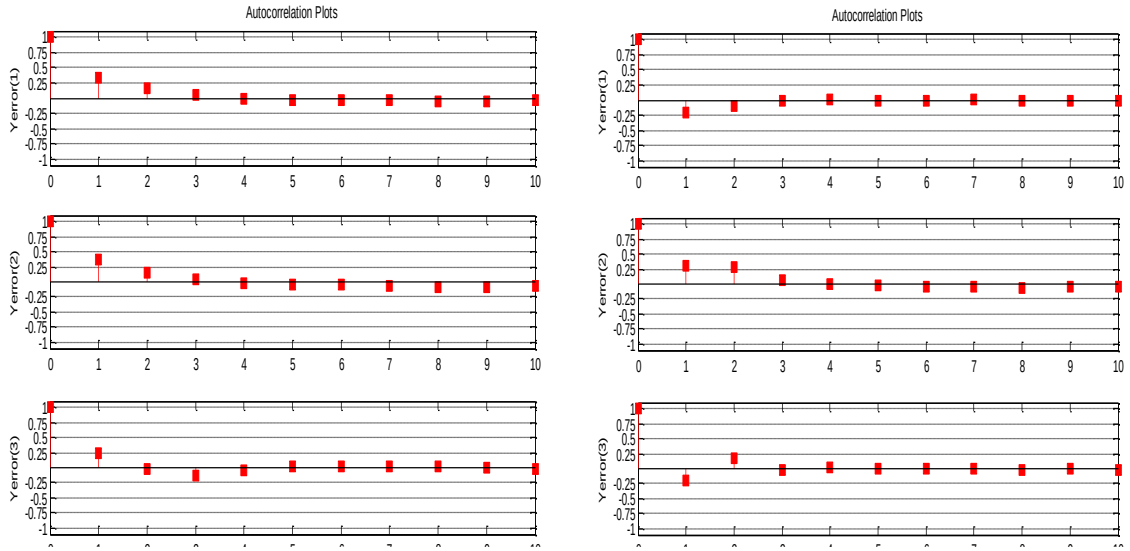

(a) (b)

Fig. 3. Autocorrelation plots of the output residuals (a) ACG state space model (b) ABCDG state space model.

The autocorrelation plots of the residuals shown in Fig. 3 reveal that both state space models produced residuals whose autocorrelation falls off steeply and is statistically zero after a lag shift of two samples. The results validate the use of the proposed state space model and estimation algorithm as a suitable alternative to the 5 matrices state space representation and Larimore's stochastic algorithm.

4. Fault monitoring statistics

Similar statistics common to those used in PCA based process monitoring can be adopted and applied for CVA state space analysis. The computation of the covariance matrices in Section 2.3 is necessary to facilitate computation of the Hotelling's T^2 statistics on the state and output residuals. Hotelling's T^2 statistics based on the first k CVA states, Eq. (51), was used by Negiz and Cinar (1997a) and Simoglou et al. (1999b). In this paper the covariance matrix of the k-dimensional state vector $\boldsymbol{\Sigma}_k$, appearing in Eq. (45), is of unity covariance for the models developed due to method of CVA employed in deriving the states. Hotelling's T^2 and Q statistics based on the residuals of the state and output matrix, as proposed by Simoglou et al. (2002), were also employed and they are given by Eq. (45) to Eq. (49).

$$T_x^2 = \mathbf{x}\boldsymbol{\Sigma}_x\mathbf{x}^\mathbf{T} \quad (45)$$

$$Q_{ey}^2 = \mathbf{e}_y\mathbf{e}_y^T \quad (46)$$

$$Q_{ex}^2 = \mathbf{e}_x\mathbf{e}_x^T \quad (47)$$

$$T_{ey}^2 = \mathbf{e}_y\boldsymbol{\Phi}_y^{-1}\mathbf{e}_y^T \quad (48)$$

$$T_{ex}^2 = \mathbf{e}_x\boldsymbol{\Phi}_x^{-1}\mathbf{e}_x^T \quad (49)$$

The control limits were established on the same statistical assumption referenced by both Negiz and Cinar (1997a) and Simoglou (1999a), that the T^2 statistics follow an F-distribution:

$$T_k^2 = \frac{k(n^2-1)}{n(n-k)}F_\alpha(k, n-k) \quad (50)$$

where n is the number of observations and $F_\alpha(k, n\text{-}k)$ is the value of the F-distribution with k and $(n - k)$ degrees of freedom for a significance level of α.

The Q statistics follow the weighted χ^2 distribution and the their control limits can be calculated as

$$\lim_\alpha = (v/2m)\chi^2_{2m^2/v,\alpha} \quad (51)$$

where m and v are the mean and variance of the statistics respectively.

5. Results of fault detection case study

5.1 The Tennessee Eastman process simulator and modelling

The proposed simplified CVA modelling approach is applied to the monitoring of the Tennessee Eastman benchmark process simulator that has been used extensively for studying process control technology and strategies and more recently process monitoring schemes. The process, as shown in Fig. 4, consists of five major unit operations: a reactor, product condenser, a vapour-liquid separator, a recycle compressor, and a product stripper. The simulated faults and a description of the open loop TE simulation is provided in Downs and Vogel (1993). The close-loop TE simulator adopted for this study is under the control strategy proposed by Lyman and Georgakis (1995). The control strategy is a plant-wide control scheme with the

control structure arranged in a multi-tiered framework in which SISO control loops are classified according to their level of importance to performance of the plant as a whole. The four tiers in order of relative importance are production and inventory control, product specification control, equipment and operating constraints, and economic performance enhancement.

Twenty one pre-programmed faults, summarized in Table 3, were tested and the fault detection delays were used to measure the monitoring performance. The data sets used were downloaded from http://brahms.scs.uiuc.edu. The statistical model was built from the normal operation data consisting of 500 samples and cross-validation was carried out using a second data set of 900 samples. All manipulated and measurement variables were used except the agitation speed of the reactor stirrer, making a total of 52 variables. The model is defined by 35 states and uses a lag order of 2 for the past and future vector. Even with the same state vector dimension, the proposed state space model provided a reduction in the number of parameters by $k(n_y + n_u)$, where k is the number of states, n_u is the number of inputs, and n_y is the number of outputs.

The eleven manipulated variables, process feeds and measured disturbance variables were all assigned as inputs variables, the remaining process variables were assigned as output variables. A comprehensive listing of the process variables and their grouping can be found in Downs and Vogel (1993).

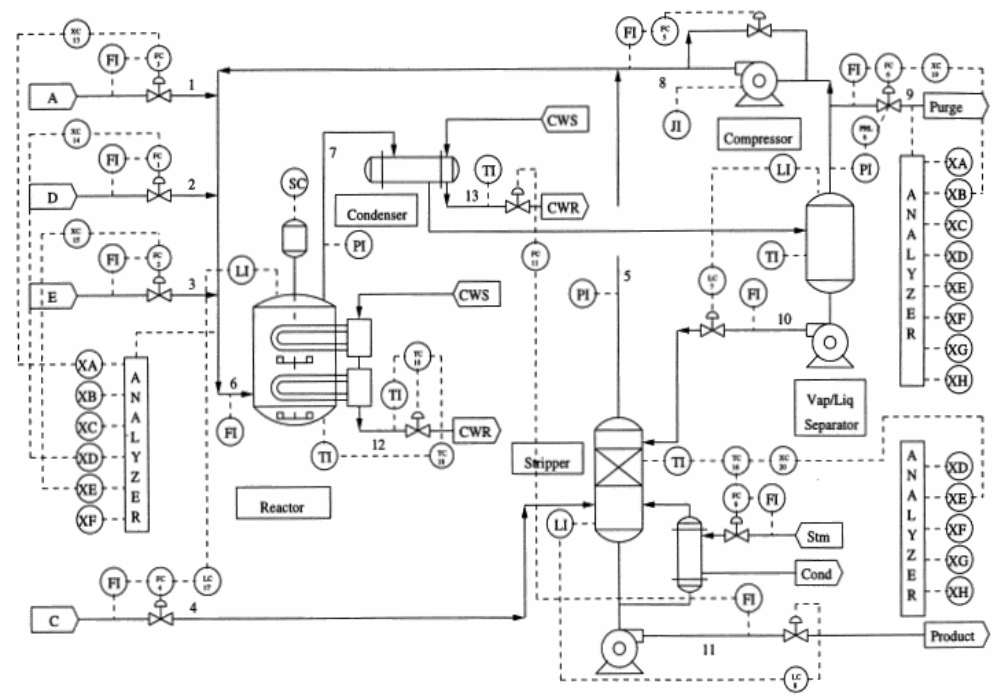

Fig. 4. Diagram of the Tennessee Eastman process simulator under Lyman and Georgakis control scheme

Table 3. List of simulated disturbances and faults

Fault	Fault Description	Fault Type
F(1)	A/C feed ratio, B composition constant (Stream 4)	Step
F(2)	B composition, A/C ratio constant (Stream 4)	Step
F(3)	D feed temperature (Stream 2)	Step
F(4)	Reactor cooling water inlet temperature	Step
F(5)	Condenser cooling water inlet temperature	Step
F(6)	A feed loss (Stream 1)	Step
F(7)	C header pressure loss- reduced availability	Step
F(8)	A, B, C feed composition (Stream 4)	Random variation
F(9)	D feed temperature (Stream 2)	Random variation
F(10)	C feed temperature (Stream 4)	Random variation
F(11)	Reactor cooling water inlet temperature	Random variation
F(12)	Condenser cooling water inlet temperature	Random variation
F(13)	Reaction Kinetics	Slow drift
F(14)	Reactor cooling water valve	Sticking
F(15)	Condenser cooling water valve	Sticking
F(16)	Unknown	
F(17)	Unknown	
F(18)	Unknown	
F(19)	Unknown	
F(20)	Unknown	
F(21)	Stream 4 valve fixed at the steady state position	Constant position

The AIC criterion proved to be most suitable for prediction of the model state order and lag-order for both the proposed and traditional state space models. The plots in the top row of Fig. 4 all show a family of AIC plots each corresponding to one of the three different complexity terms discussed earlier (Eq. 41 – 43). The AIC plots are shown to be less sensitive to the choice of complexity term and all the plots fairly followed each other in terms of parabolic fitness. However, the fix size lag/lead order employed for the dynamic expansion to construct the past and future matrices is shown to be of more influence on the model selection criterion. In the end, a lag order ***L*** of 2 gave AIC curves with minimum points most consistent with the state order return by the MSE plots shown in the bottom row of Fig. 4 and the state order as determine by the algorithm proposed in Section 3. The lag order of two also corresponds to the minimum MSE attainable as can be observed from the various plots.

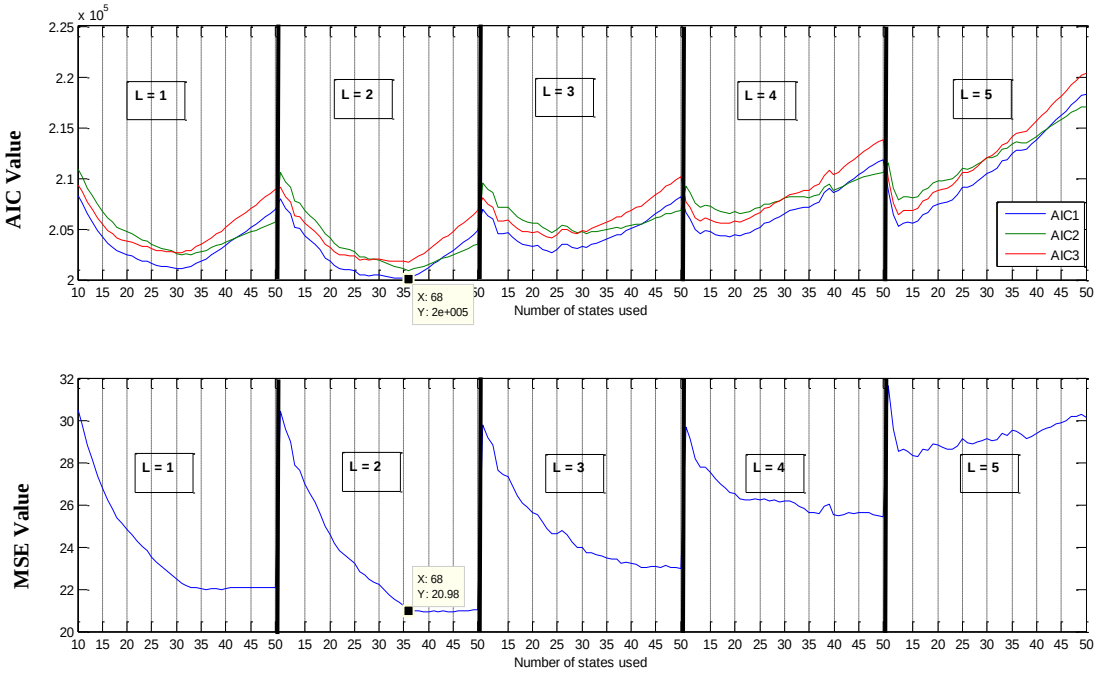

AIC1 – Eq. 41 AIC2 – Eq. 42 AIC2 – Eq. 43

Fig. 5 AIC and MSE computation for the monitoring-specific SS models (ABC) spanning lag size from 1 to 5 and state order from 10 to 50.

Both the BIC and LLIC failed to converge and indicate the true state order for the model as can be observed in Fig. 6. The LLIC plots generate parabolic shape curves but the minimum points of the curve can be observed to be achieved at a much lower-sate order in comparison to the state order observed by both the AIC and MSE plots of Fig. 5.

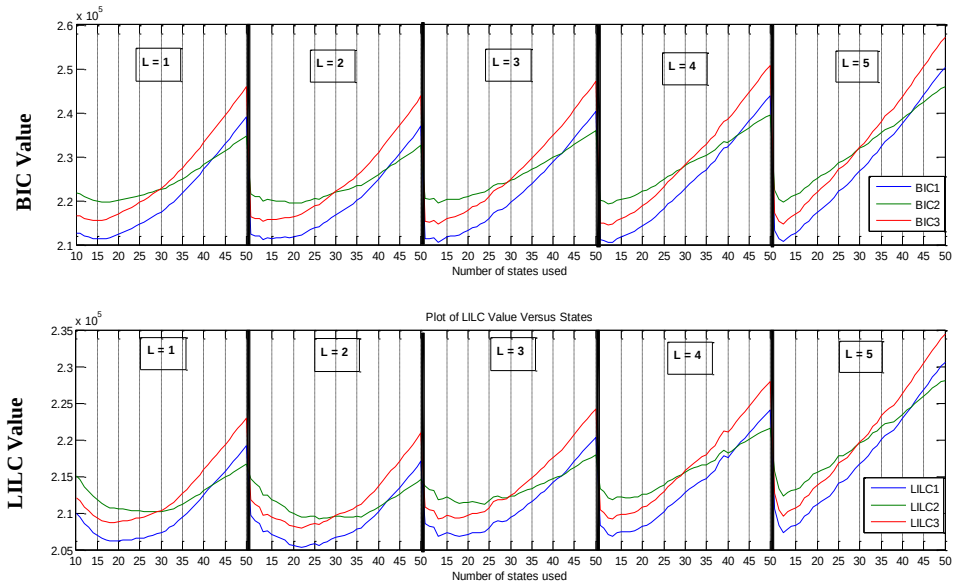

BIC1/LILC1 – Eq. 41 **BIC2/LILC2 – Eq. 42** **BIC2/LILC2 – Eq. 43**

Fig. 6 BIC and LILC computation for the monitoring-specific SS models (ABC) spanning lag size from 1 to 5 and state order from 10 to 50.

5.2 Fault monitoring results

The two CVA state space models were developed using MATLAB. Based upon the computation complexity equations provided in Table 1, the dimension of the training data set along with the number of state variables used to define models, the required number of FLOPS was 6.58×10^6 for computation of 5 matrices state space representation and 2.53×10^6 for the proposed state space model. The numbers were consistent with the algorithms computation time recorded in MATLAB. Though the computation time was found to vary from run to run, the computation time for the proposed model was consistently less, ranging from 29% to 54% of the computational time recorded for the traditional CVA model development. The variation in the

recorded computational times was attributed to fluctuation in the available processing power due to demand from other background processes relating to other applications that were running on the machine.

Table 4. Detection delay times of the proposed CVA model with previously reported results.

	Delay	Statistics	PCA T^2	PCA Q	DPCA T^2	DPCA Q	CA Q	CA T^2
F1	**3**	T^2_{ey},T^2_{ex}	21	9	18	15	6	33
F2	**12**	T^2_{ey}	51	36	48	39	33	36
F4	**3**	T^2_{ey},T^2_{ex},Q_{ey}	F	9	453	3	3	F
F5	**3**	All	48	**3**	6	6	3	27
F6	**3**	All	30	**3**	33	**3**	**3**	24
F7	**3**	All	**3**	**3**	**3**	**3**	**3**	**3**
F8	**24**	T^2_{ey}	60	60	69	63	60	87
F10	**72**	Q_{ey}	288	147	303	150	81	186
F11	**18**	T^2_{ey},Q_{ex}	912	33	585	**21**	33	567
F12	**3**	T^2_{ey},T^2_{ex}	66	24	9	24	9	63
F13	**90**	T^2_{ey}	147	111	135	120	123	147
F14	**3**	T^2_{ey},T^2_{ex},T^2_{x},Q_{ey}	12	**3**	18	**3**	**3**	F
F15	**30**	T^2_{ey}	F	F	F	F	F	F
F16	**18**	T^2_{ey}	936	591	597	588	30	108
F17	**48**	T^2_{ey}	87	75	84	72	66	468
F18	228	T^2_{ey}	279	252	279	252	**225**	288
F19	**6**	Q_{ex}	F	F	F	246	441	F
F20	**189**	T^2_{ey}, Q_{ex}	261	261	267	252	222	252
F21	**765**	T^2_{x}	1689	855	1566	858	780	1527

Hotelling's T^2 and Q statistics on output residuals: T^2_{ey}/Q_{ey}; Hotelling's T^2 and Q statistics on state residuals: T^2_{ex}/Q_{ex}; Hotelling's T^2 statistics on the state variables: T^2_{X}.

Table 4 summarizes and compares the results obtained from the simulation runs and compares the fault detection delay time of the best performing monitoring statistics of the proposed model with previously published results of other statistical methods: correspondence analysis (CA) and (dynamic) principal component analysis (PCA and DPCA) carried out on the same data sets, see Russell et al. (2000) and Detroja et al. (2007). The detection delay is expressed as the time delay in number of samples between fault introduction and its detection. In Table 4, the best performance is marked as bold font. The label "F" in Table 4 indicates that the fault was not detected. The statistics and model giving the quickest detection for a given fault is

highlighted in bold in the table. Fault detection using the proposed CVA model not only detected faults quicker in most cases but was also able to detect faults (e.g. F15) for which the other models were not able to flag. The five monitoring statistics given in Eq. (45) to Eq. (49) were applied independently and the best performing detection statistics for each fault case was noted.

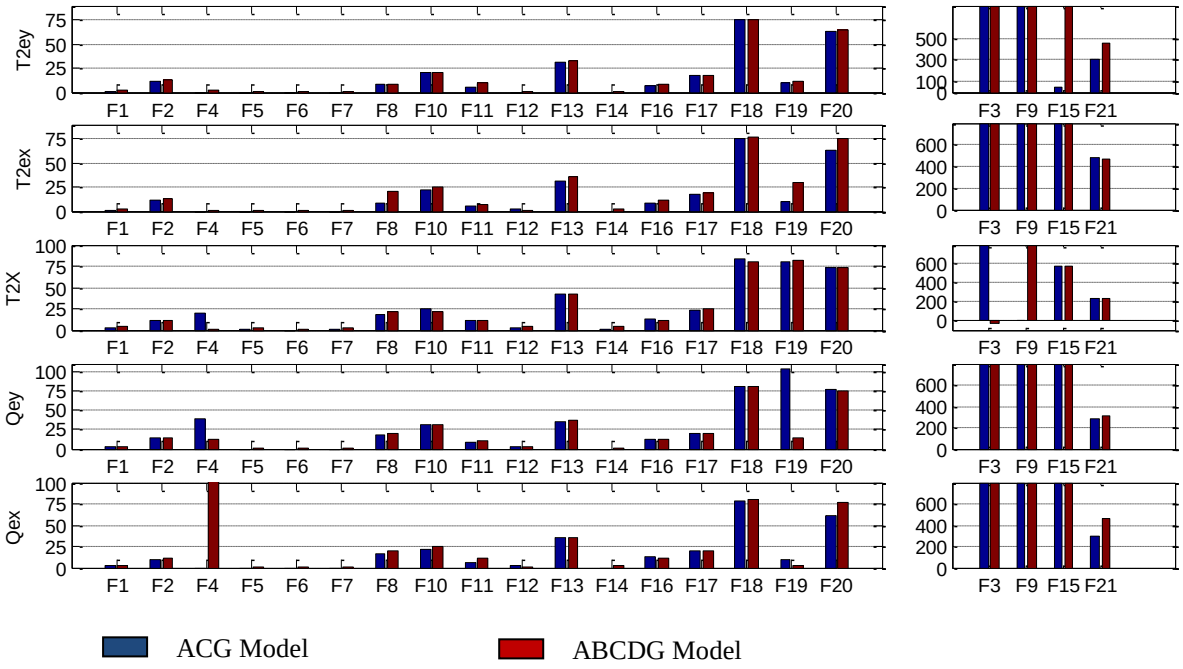

Fig. 7. Fault detection delay time comparison of the 5 monitoring statistics across the 2 CVA state space models. Missing bars indicate zero detection delay time, negative bars indicate false alarm condition and full length bars indicate failed/missed detections.

The bar charts in Fig. 7 compare the fault detection performance of the proposed CVA based state space model (ACG) with Larimore's CVA based state space model (ABCDG). Some faults were readily detectable while others proved more difficult to detect or undetectable and this general categorization is differentiated in Fig. 7. The undetectable or more difficult to detect faults are grouped and shown to the left-hand-side of the figure (Faults 3, 9, 15, and 21).

The performance of the proposed model is for the most part on par or in some cases slightly better than Larimore's state space model. Again, the Hotelling's statistics on the output error T_{ey}^2 was able to give early detection on Fault No. 15 (cool

water valve sticking), see Fig. 8. The detection of this particular fault was not achievable by other statistical methods including Larimore's CVA state space modelling technique. The Q statistics based on the proposed CVA model also provided modest improvement in the detection of Faults 20 and 21.

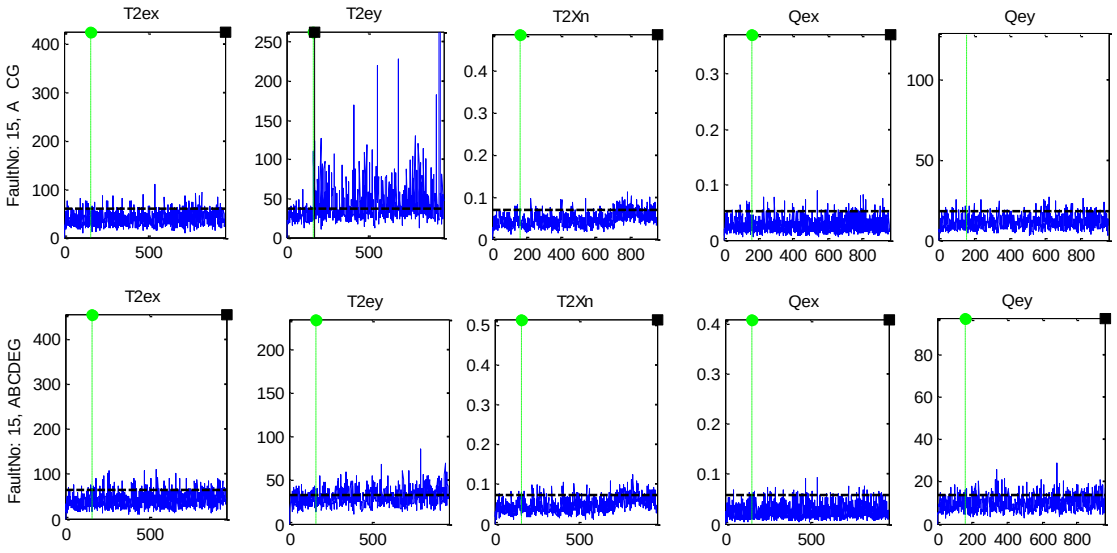

Fig. 8. Detection of fault No. 15 using ACG and ABCDG state space models

A more recent publication (Odiowei and Cao, 2010) also conducted a comparative analysis of their proposed state space independent component analysis SSICA approach against the performance of the CVA and dynamic independent component analysis DICA approach. The SSICA is essentially a combination of a first stage CVA state space model and a second stage independent component analysis ICA approach. The authors attributed the improved performance of SSICA over the usual DICA approach due to the fact that CVA SS model is better suited for capturing the dynamics of a process than a dynamic principal component analysis DPCA method upon which DICA is based. ICA method is said to be better suited for process characterised by non-Gaussian distribution.

Both detection delay times and percentage reliability metrics were analysed, Table 5 compares extracts of their results with the fault monitoring performance of the proposed CVA state space performance. The percentage reliability is defined as the percentage of the samples outside the control limits. The proposed model

outperformed or detected on par with the SSICA/DICA method in terms of detection delay time for faults 1, 2, 4, 5, 6, 7, 11, 12, 13, 14, 16, 17 and 19 but performed inferior for the remaining faults not including fault 21 which was not included in Odiowei and Cao (2010) fault simulation and analysis study.

Table 5. Fault detection performance comparison of CVA versus DICA and SSICA

	Detection Delay time (min)			Detection Reliability (%)		
Fault	CVA*	DICA	SSICA	CVA*	DICA	SSICA
1	3	9	9	98.58	99.75	99.75
2	12	15	12	99.44	99.50	99.63
3	-	21	15	-	19.48	73.03
4	3	6	6	99.80	99.88	99.88
5	3	6	6	99.88	99.88	99.88
6	3	6	6	99.90	99.88	99.88
7	3	6	6	98.61	99.88	99.88
8	24	33	18	98.52	98.75	99.88
9	-	48	18	-	46.82	91.64
10	72	96	18	97.54	96.13	96.75
11	18	18	18	99.44	99.38	99.38
12	3	15	15	99.58	99.50	99.50
13	90	96	18	97.60	96.13	96.25
14	3	6	6	98.57	99.88	99.88
15	30	15	12	99.68	99.50	99.63
16	18	21	18	98.75	99.25	99.38
17	48	48	18	98.75	98.13	98.38
18	228	21	21	99.80	99.25	99.25
19	6	6	6	98.57	99.88	99.88
20	189	72	18	98.61	97.13	97.63

In particular, Odiowei and Cao (2010) have reported successful detection of faults # 3 and # 9 with relatively high reliability. Based on the authors' literature review, no other publications have reported achieving such. Beside these two faults,

the fault detection reliability was above 97% for all detectable faults for the proposed CVA state space model and therefore gave an overall better fault performance than both the DICA and SSICA schemes in that regards.

The detection performance of a given fault detection scheme (model and statistics) is dependent upon both components of the system. A particular parameterization of a model may favour detection of certain types of fault over others. Hence, for some faults analysed, the detection delay time was sensitive to specification of the model in terms of state vector dimension and lead/lag window size.

6. Conclusions

A simplified CVA based state-space model design for the specific purpose of process monitoring was achieved using a simpler and more efficiently estimation of a reduced set of state space parameter matrices. The performance integrity of the state space model was maintained in conjunction with a dramatic reduction in the number of model parameters and simplification of the set of stochastic estimation equations used to derive the model parameters. Application results on the Tennessee Eastman benchmark process indicate that the proposed state space representation and model development technique provides comparable, and in many cases better, fault detection performance than the traditional CVA state space modelling technique. Most notable is the detection of fault No. 15 in the Tennessee Eastman benchmark process and the significant reduction in detection delay time achieved for the more difficult to detect faults. The overall best performing monitoring statistics in terms of fault detection and detection delay time is the Hotelling's T^2 statistics of the output residuals T^2_{ey}.

The fault detection performance also faired comparably to that reported for the DICA and SSICA schemes (Odiowei and Cao, 2010) save for the unprecedented detection of faults 3 and 9. However, for those faults detectable by the proposed CVA method, the percentage performance reliability was better on average than that of DICA and SSICA. Future research could explore what further fault performance improvements could be yield from combining the ICA approach with a CVA state space model as proposed in this paper. Diagnosis or isolation of faults including

multiple simultaneous faults based on CVA state space model will be investigated in the future.

Acknowledgements

The work is supported by Dorothy Hodgkin Postgraduate Award and BP International Ltd.

References

Akaike, Hirotugu. 1975. Markovian Representation of Stochastic Processes by Canonical Variables. *Society of Industrial and Applied Mathematics - SIAM J Control* 13 (1): 162-173.

Brown, R. G., and Hwang, P. Y. C. (1992). Introduction to Random Signals and Applied Kalman Filters, 2nd ed., John Wiley and Sons, Inc.

Candy, J. V., Bullock T. E., and Warren M. E. 1979. Invariant Description of the Stochastic Realization. *Automatica* 15: 493-495.

Detroja, K. P., R. D. Gudi, and S. C. Patwardhan. 2007. Plant-wide detection and diagnosis using correspondence analysis. *Control Engineering Practice* 15 (12): 1468-1483.

Downs, J. J., and E. F. Vogel. 1993. A PLANT-WIDE INDUSTRIAL-PROCESS CONTROL PROBLEM. *Computers & Chemical Engineering* 17 (3): 245-255.

Juricek, B. C., W. E. Larimore, and D. E. Seborg. 1999. Reduced-rank ARX and subspace system identification for process control. *Dynamics & Control of Process Systems 1998, Volumes 1 and 2*: 247-252.

Juricek, B. C., D. E. Seborg, and W. E. Larimore. 2005. Process control applications of subspace and regression-based identification and monitoring methods. *ACC: Proceedings of the 2005 American Control Conference, Vols 1-7*: 2341-2346.

Larimore, Wallace E. 1983. System Identification, Reduced Order Filtering and Modelling via Canonical Variate Analysis. *Proceedings from American Control Conference* 2: 445 - 451.

Larimore, Wallace E. 1990. Canonical Variate Analysis in Identification Filtering and Adaptive Control. *Proceedings of the 28th Conference on Decision and Controls*: 596-604.

Lee, C., S. W. Choi, and I. B. Lee. 2006. Variable reconstruction and sensor fault identification using canonical variate analysis. *Journal of Process Control* 16 (7): 747-761.

Lyman, P. R., and C. Georgakis. 1995. Plant-Wide Control of the Tennessee Eastman Problem. *Computers & Chemical Engineering* 19 (3): 321-331.

Negiz, A., and A. Cinar. 1997a. Statistical Monitoring of Multivariable Dynamic Processes with State Space Models. *AICHE* 43 (8): 2002-2020.

Negiz, A., and A. Cinar. 1997b. Pls, balanced, and canonical variate realization techniques for identifying VARMA models in state space. *Chemometrics and Intelligent Laboratory Systems* 38 (2): 209-221.

Odiowei, P. P., and Y. Cao. 2010. State-space independent component analysis for nonlinear dynamic process monitoring. *Chemometrics and Intelligent Laboratory Systems* 103 (1): 59-65.

Russell, E. L., L. H. Chiang, and R. D. Braatz. 2000. Fault detection in industrial processes using canonical variate analysis and dynamic principal component analysis. *Chemometrics and Intelligent Laboratory Systems* 51 (1): 81-93.

Schaper, C. D., W. E. Larimore, D. E. Seborg, and D. A. Mellichamp. 1994. IDENTIFICATION OF CHEMICAL PROCESSES USING CANONICAL VARIATE ANALYSIS. *Computers & Chemical Engineering* 18 (1): 55-69.

Simoglou, A., E. Martin, and J. Morris. 1999a. A Comparison of Canonical Variate Analysis and Partial Least Squares for the Identification of Dynamic Processes. *Proceedings from American Control Conference* 2: 832 - 837.

Simoglou, A., E. B. Martin, and A. J. Morris. 1999b. Dynamic multivariate statistical process control using partial least squares and canonical variate analysis. *Computers & Chemical Engineering* 23: S277-S280.

Simoglou, A., E. B. Martin, and A. J. Morris. 2002. Statistical performance monitoring of dynamic multivariate processes using state space modelling. *Computers & Chemical Engineering* 26 (6): 909-920.

Yao, Y., and F. Gao. 2008. Subspace identification for two-dimensional dynamic batch process statistical monitoring. *Chemical Engineering Science* 63 (13): 3411-3418.